IL NUOVO CIMENTO Vol. 24 C, N. 4-5 Luglio-Ottobre 2001

Experimental results on cosmic ray composition and energy spectrum around the knee from EAS experiments(*)

A. Castellina

Istituto di Cosmogeofisica del CNR - C.so Fiume 4, 10133 Torino, Italy

(ricevuto il 14 Novembre 2000; approvato il 12 Febbraio 2001)

Summary. — The most recent experimental results on cosmic ray composition and energy spectrum from Extensive Air Shower arrays are reviewed and discussed. All experiments agree on the presence of the knee in the energy spectrum at an energy $E_k \simeq 3 \cdot 10^{15}$ eV; the bend is seen in all the shower components, whose study gives consistent results and do not suggest any change in hadronic interactions at these energies. An astrophysical origin for the knee is thus favoured. Most experiments agree on a primary mass composition getting heavier above the knee, but contradicting data also exist. In particular the results based on the observation of the atmospheric Čerenkov light, the component more strictly related to the total primary energy, seem to suggest an opposite trend.

PACS 95.55.Vj – Neutrino, muon, pion, and other elementary particle detectors; cosmic ray detectors.
PACS 96.40.De – Composition, energy spectra, and interactions.
PACS 96.40.Pq – Extensive air showers.
PACS 01.30.Cc – Conference proceedings.

1. – Introduction

The experimentally observed cosmic ray energy spectrum is well described by a power law, which steepens around $3 \cdot 10^{15}$ eV, a feature called the "knee", firstly discovered in 1958 [1], and which softens again at $\simeq 10^{19}$ eV, the "ankle". It is widely believed that cosmic rays at least up to the knee energy are confined in the Galaxy; they are accelerated by diffusive shocks in Supernova remnants up to a maximum energy near the knee, which could either correspond to the maximum achievable energy in the accelerator or could be due to propagation effects. Another possible interpretation connects the knee to a possible change in the hadronic interaction properties at such high energy. From the experimental point of view, what is most important in order to test the models is to

(*) Paper presented at the Chacaltaya Meeting on Cosmic Ray Physics, La Paz, Bolivia, July 23-27, 2000.

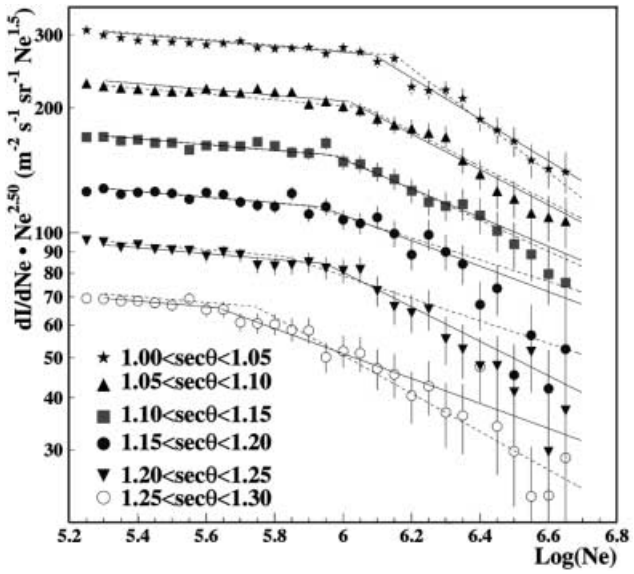

Fig. 1. – Differential electron size spectrum at different atmospheric depths from EAS-TOP [3].

measure the cosmic ray composition and energy spectrum near the energy limit of the shock models; moreover, measurements of anisotropy and secondary to primary ratio at higher energy are of utmost importance.

Direct measurements of the primary spectrum and mass require instrumentation being flown on balloons or satellites; unfortunately, because of the rapidly falling energy spectrum, they are restricted to energies below the knee and only indirect methods can be exploited above, where the flux is less than 1 particle m^{-2} y^{-1}.

The interpretation of these ground level observations in terms of primary particle characteristics is however far from straightforward, being strongly dependent on models simulating the production and propagation of particles through the atmosphere, which in turn depend on extrapolations applied to available data from p-$\overline{p}$, e-p and heavy-ion accelerators.

The most recent results of EAS experiments concerning the primary energy spectrum and the mass composition of cosmic rays are described in the following.

2. – Charged-particle detectors

The experimental observables we are dealing with are the charged components of showers as measured by ground-based detectors: electrons, muons and hadrons.

The electron and muon size spectra as measured by the EAS-TOP experiment [2] are shown in fig. 1 and fig. 2. The shower size at the knee decreases with increasing atmospheric depth, as expected for a feature of the primary spectrum, with an attenuation length $\Lambda_k = (222 \pm 3)$ g cm^{-2}, in very good agreement with that found for the shower absorption in the atmosphere [3].

The integral fluxes in electron and muon size are compatible at all atmospheric depths, as expected for a feature occurring at fixed primary energy, also confirming the consistency of the whole procedure. A simulation of the shower production and development

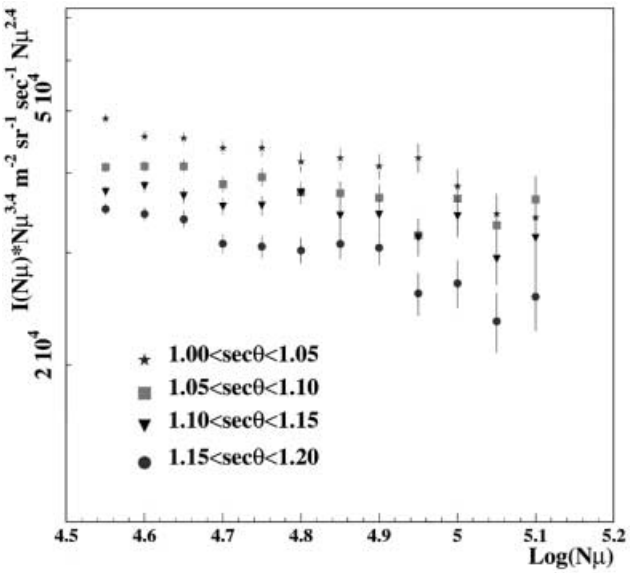

Fig. 2. – Differential muon size spectrum at 4 different atmospheric depths as measured by EAS-TOP [3].

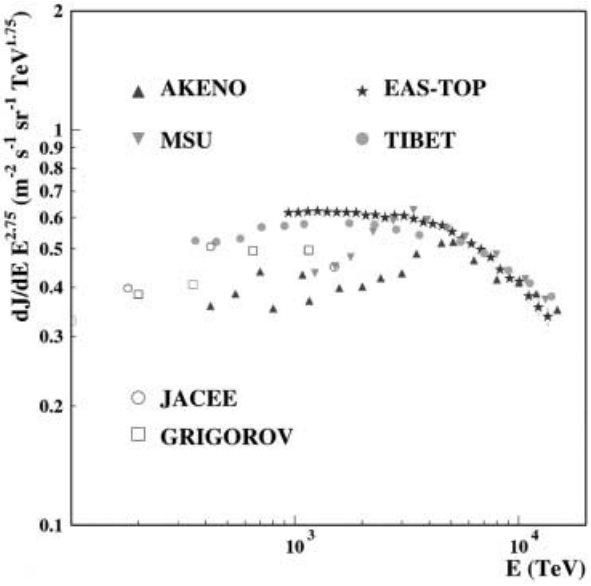

Fig. 3. – Primary energy spectrum as measured by EAS-TOP compared with other experimental results [3].

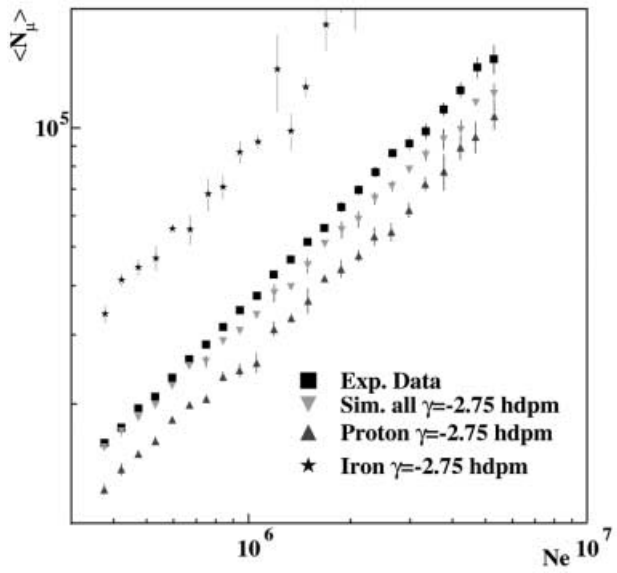

Fig. 4. – $\langle N_\mu \rangle$ *vs.* N_e from EAS-TOP as compared to a simulation with constant composition [5].

in atmosphere using the CORSIKA code [4] with the HDPM interaction model was used to find the relation between shower size and primary spectrum $N_\mathrm{e} = \alpha(A_\mathrm{eff})E^{\beta(A_\mathrm{eff})}$. The effective mass A_eff is calculated from the extrapolation of the single nuclear spectra measured at low energies by direct measurements; above the knee, a rigidity dependent cutoff is used. The final result is shown in fig. 3; the agreement with direct measurements at low energies and with other EAS experimental results at the highest ones is quite good. A 10% systematic uncertainty in all the particle flux comes from the choice of A_eff; different hadronic interaction models would give a value for N_e different by $\simeq 10\%$ from the HDPM one at 2×10^{15} eV.

The EAS-TOP group studied the composition by analyzing the behaviour of $\overline{N_\mu}$ as measured in vertical direction in narrow bins of N_e, corresponding to $\Delta N_\mathrm{e}/N_\mathrm{e} = 12\%$ [5]. The result is shown in fig. 4, where data are compared with the results of a full simulation including the detector response and the 1 TeV composition with equal slopes for all components was used, in this way assigning a composition independent of energy. The EAS-TOP data clearly suggest a growth of the mean A with energy, that is a heavier composition above the knee. A change of $\Delta \log(N_\mathrm{e}) = 0.5$ results in a $\Delta A/A = 0.4$.

The muon and electron (actually the sum of e^-, e^+, γ's) size measurements are used in a quite different way by the CASA-MIA group [6] to determine the energy spectrum. They found in fact that the sizes combination $F = \log_{10}(N_\mathrm{e}^* + \psi N_\mu)$ is log-linear in E_0 and, what is most important, it does not depend on the primary mass. The systematic differences in energy assignment for different primary mass values are less than 5%. The energy spectrum thus derived is shown in fig. 5; it is characterised by a smooth transition across the knee, which is located at the same primary energy, as expected.

Using the electron and muon densities at different distances from the core and the slope of the electron lateral distribution function near the core, the CASA-MIA group generated samples of events for each different primary mass by Monte Carlo. An experimental event is assigned to the "light primary" or "heavy primary" class by looking at

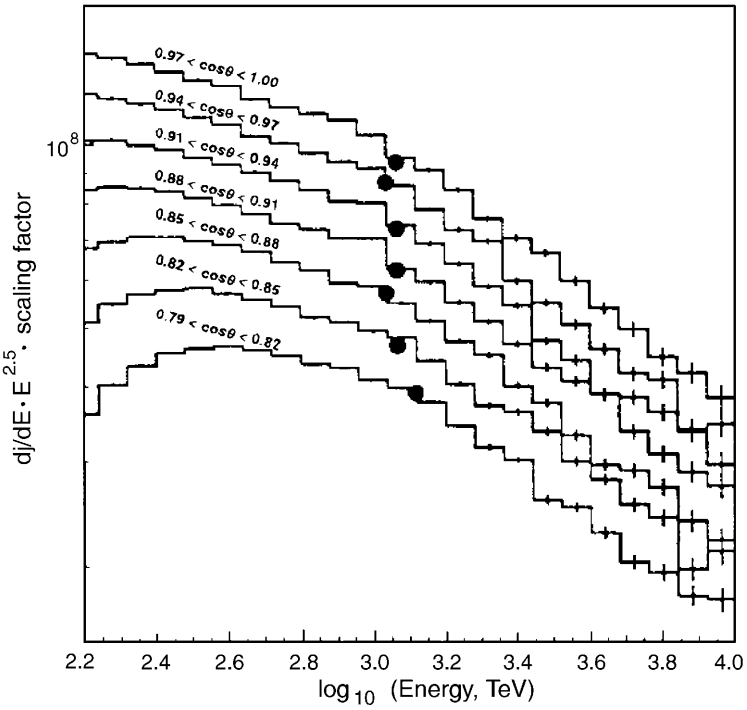

Fig. 5. – Primary energy spectrum as measured by CASA-MIA [6].

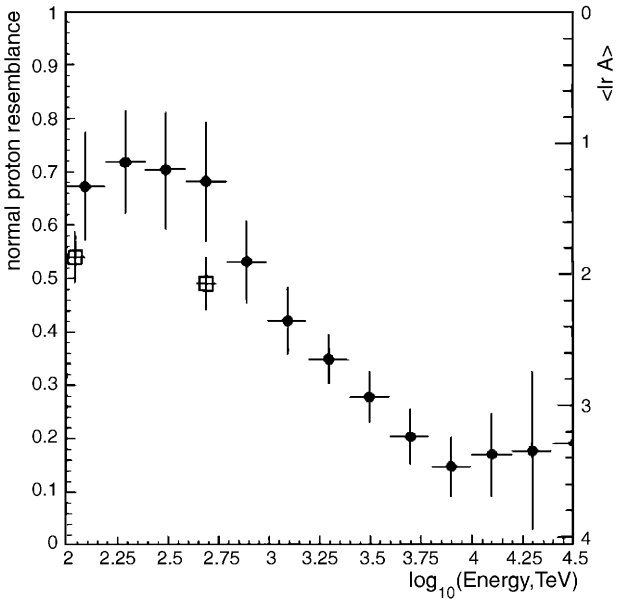

Fig. 6. – Proton resemblance plot for CASA-MIA [7].

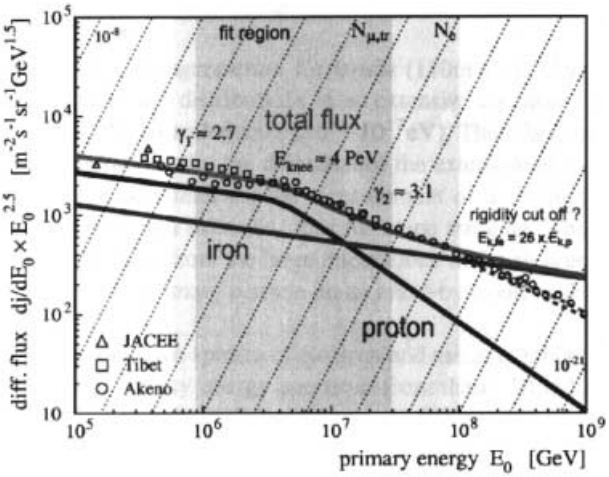

Fig. 7. – Primary energy spectrum by KASCADE from the electron and muon size spectra [10].

the K nearest neighbours (KNN) in the plane of the used variables [7] ; Monte Carlo in fact shows that most of the neighbours are of the same species of the considered events in more than 90% of the cases. Fluctuations are however quite big and classes tend to superimpose; thus only broad classes of "p-like" and "Fe-like" events can be used; anyway, the experimental data show a clear trend towards a heavier composition above the knee. The average fraction of KNN which are protons (the "proton resemblance") is approximately proportional to $\langle \ln A \rangle$ and it is shown in fig. 6 for $K = 5$.

KASCADE [8] studied the spectrum and composition of cosmic rays using all the three measured charged components of EAS: electrons, muons and hadrons. The knee is clearly visible in all components and again the size at the knee decreases at increasing atmospheric depth [9]. In fig. 7, the energy spectrum is found by a combined χ^2 minimisation to fit both the N_e and the N_μ^{tr} truncated muon size spectra simultaneously [10]. The light component is responsible for the knee, while data suggest a rigidity cut-off at $E_{k,Fe} \simeq 26 \times E_{k,p}$ for the iron one.

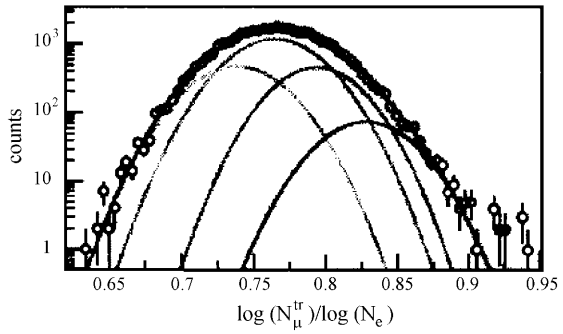

Fig. 8. – $\log N_\mu^{tr} / \log N_e$ for one energy bin ($6.2 \leq \log(E/\mathrm{GeV}) \leq 6.3$) [11]. Four simulated distributions for p, He, O, Fe primaries are shown from left to right, respectively.

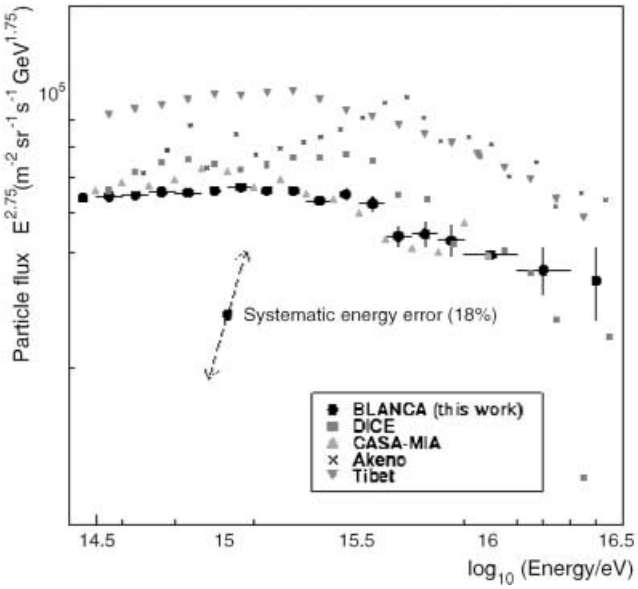

Fig. 9. – Primary energy spectrum from BLANCA ([12] and references therein).

The most sensitive dependence on primary mass was identified by KASCADE in the ratio $\log N_\mu^{\mathrm{tr}} / \log N_{\mathrm{e}}$, which is Gaussian distributed at fixed A [11]. The experimental ratio is fitted by a superposition of simulated distributions (one for each primary mass group), directly obtaining the fraction of each mass groups, as shown in fig. 8. The composition is dominated by the light component up to about 4 PeV, getting heavier above the knee; the analysis also proves that the composition cannot be described by a single component.

3. – Čerenkov detectors

The broader lateral distribution of the Čerenkov light and the high photon number density are the main advantages of using Čerenkov detectors as compared to charge particle counting arrays.

BLANCA [12] consists of 144 angle-integrating Čerenkov light detectors located in the CASA scintillator array and measures the Čerenkov lateral distribution function; the intensity at a critical radial distance of 120 m, entirely determined by density and scale height of the atmosphere, is proportional to the primary energy and the dependence on the primary mass is fully included in the slope s of the distribution, which is in fact a function of the depth of maximum development $X_{\max}$.

In experiments like BLANCA, Spase-VULCAN [13], CACTI [14], Hegra-AIROBICC [15], $X_{\max}$ is measured from the slope of the Čerenkov lateral distribution, which is an almost linear function of the depth of shower maximum. The function relating the slope to the depth of maximum development is rather independent of the models chosen to describe the hadronic interactions, while any interpretation of the experimental result in terms of primary composition is not.

In DICE [16], 2 imaging telescopes of 2 m diameter are employed. They measure

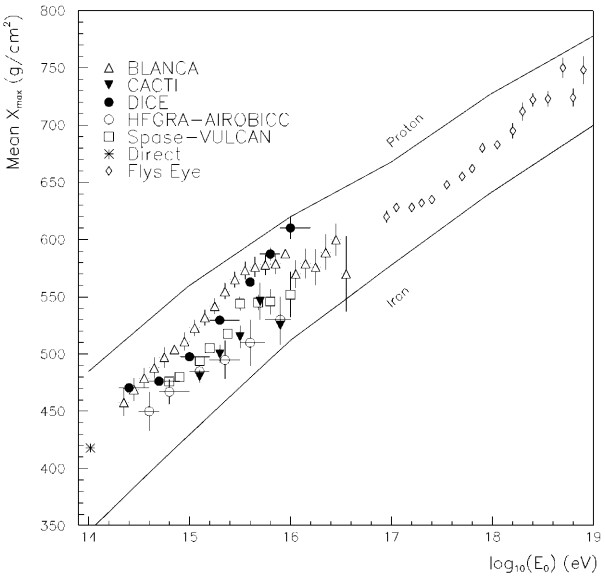

Fig. 10. – Mean depth of shower maximum *vs.* energy.

the Čerenkov light size N_γ, by summing the total amount of light at each PM, and the depth of maximum development of the shower $X_{\max}$, by fitting the shape of the light image in each telescope. The imaging technique allows to measure $X_{\max}$ in a rather direct way; the procedure is essentially geometrical and does not depend on simulation, except for calculations to determine the angular distribution of light around the axis. The primary energy is estimated through a fit including geometry, N_γ and $X_{\max}$ and takes therefore into account the dependence of the lateral distribution and intensity of the Čerenkov light, at fixed primary energy, on the primary mass. The resulting energy spectra from BLANCA and DICE are shown in fig. 9, compared with other experimental results. BLANCA finds a knee as wide as half a decade in energy; a systematic energy error of $\simeq$ 18% would affect the flux as indicated by the diagonal arrows. According to DICE data, the knee is found around 3 PeV; a $\simeq$ 30% systematic uncertainty in the flux comes from the intrinsic uncertainty in the energy scale. The DICE result has also been confirmed by a correlated analysis using DICE and CASA-MIA data [16]; a primary composition becoming pure iron above the knee was excluded.

A survey of the results in the measurement of $X_{\max}$ is shown in fig. 10, up to the Fly's Eye energies (where air fluorescence is measured) [17]; the "direct" point shows the $X_{\max}$ that would be expected on the basis of balloon direct measurements [18]. A comparison with expectations from CORSIKA+QGSJET [19] shows a trend of data towards a lighter composition across the knee.

4. – Conclusion

The energy spectrum and composition of primary cosmic rays have been studied employing different techniques measuring various air shower components. The knee in the primary spectrum of cosmic rays has been observed in all the shower components at an energy of $\simeq$ 3–4 PeV; the astrophysical interpretation of the knee is thus favoured.

Most data show an increase in the average primary mass across the knee, even if the absolute scale in $\langle \ln A \rangle$ is quite different, depending on which observables are used to extract the information. However, considering the data from Čerenkov experiments, the composition shows an opposite trend, although BLANCA data suggest that it become heavier again after the knee. A broader summary of the up-to-date situation is given in [20], where a survey of data in terms of $\langle \ln A \rangle$ is also presented.

Possible explanations of the large spread in the results can be found by comparing the different sensitivity to composition of the various observables and the different ways used to determine the primary energy by various groups. A deeper understanding both of the hadronic interaction models (see, *e.g.*, [21]) and of the systematics, which could bias the results, is also needed.

REFERENCES

[1] Kulikov G. V. and Khristiansen G. B., *Sov. Phys. JETP*, **8** (1959) 41.
[2] Aglietta M. *et al.*, *Nucl. Instrum. Methods A*, **336** (1993) 310.
[3] Aglietta M. *et al.*, *Astropart. Phys.*, **10** (1999) 1.
[4] Heck D. *et al.*, Report FZKA 6019, Forschungzentrum Karlsruhe (1998).
[5] Aglietta M. *et al.*, *Proceedings of the 26th ICRC (Salt Lake City)*, vol. **1** (1999) p. 230.
[6] Glasmacher M. A. K. *et al.*, *Astropart. Phys.*, **10** (1999) 291.
[7] Glasmacher M. A. K. *et al.*, *Astropart. Phys.*, **12** (1999) 1.
[8] Klages H. O. *et al.*, *Nucl. Phys. B, Proc. Suppl. B*, **52** (1997) 92.
[9] Kampert K. H. *et al.*, *Second Meeting on New Worlds in Astroparticle Physics, University of Algarve, Faro, Portugal* (1998).
[10] Glasstetter R. *et al.*, *Proceedings of the 26th ICRC (Salt Lake City)*, vol. **1** (1999) p. 222.
[11] Weber J. H. *et al.*, *Proceedings of the 26th ICRC (Salt Lake City)*, vol. **1** (1999) p. 341.
[12] Fowler J. W. *et al.*, astro-ph/0003190.
[13] Dickinson J. E. *et al.*, *Nucl. Instrum. Methods A*, **440** (2000) 114.
[14] Paling S. *et al.*, *Proceedings of the 25th ICRC (Durban)*, vol. **5** (1997) p. 253.
[15] Röhring A. *et al.*, *Proceedings of the 26th ICRC (Salt Lake City)*, vol. **1** (1999) p. 214.
[16] Swordy S. P. and Kieda D. B., *Astropart. Phys.*, **13** (2000) 137.
[17] Bird D. *et al.*, *Phys. Rev. Lett.*, **71** (1993) 3401.
[18] Swordy S. P., *Proceedings of the 23rd ICRC (Calgary)*, Invited and Rapporteur papers (1993) p. 243.
[19] Pryke C., Auger GAP Note 98-035, FNAL (1998).
[20] Castellina A., *Proceedings of the XI International Symposium on Very High Energy Cosmic Ray Interactions, Campinas (2000)*, *Nucl. Phys. B (Proc. Suppl.)*, **97** (2001) 35.
[21] Antoni T. *et al.*, *J. Phys. G*, **25** (1999) 2161.